Two species drag/diffusion model for energetic particle driven modes

V. Aslanyan, S. E. Sharapov, D. A. Spong, and M. Porkolab

Citation: Physics of Plasmas **24**, 122511 (2017);
View online: https://doi.org/10.1063/1.4996123
View Table of Contents: http://aip.scitation.org/toc/php/24/12
Published by the American Institute of Physics

Two species drag/diffusion model for energetic particle driven modes

V. Aslanyan,[1] S. E. Sharapov,[2] D. A. Spong,[3] and M. Porkolab[1]
[1]*MIT PSFC, 175 Albany Street, Cambridge, Massachusetts 02139, USA*
[2]*CCFE, Culham Science Centre, Abingdon OX14 3DB, United Kingdom*
[3]*Oak Ridge National Laboratory, Oak Ridge, Tennessee 37831-6169, USA*

(Received 14 July 2017; accepted 28 November 2017; published online 19 December 2017)

A nonlinear bump-on-tail model for the growth and saturation of energetic particle driven plasma waves has been extended to include two populations of fast particles—one dominated by dynamical friction at the resonance and the other by velocity space diffusion. The resulting temporal evolution of the wave amplitude and frequency depends on the relative weight of the two populations. The two species model is applied to burning plasma with drag-dominated alpha particles and diffusion-dominated ICRH accelerated minority ions, showing the stabilization of bursting modes. The model also suggests an explanation for the recent observations on the TJ-II stellarator, where Alfvén Eigenmodes transition between steady state and bursting as the magnetic configuration varied. *Published by AIP Publishing*. https://doi.org/10.1063/1.4996123

I. INTRODUCTION

Instabilities driven by the energetic particles in fusion plasmas[1] are of significant concern for the next-step burning plasma experiment as these instabilities may affect the alpha-particle heating profile, helium ash accumulation, and cause damage to the first wall.[2,3] The nonlinear temporal evolution of the instabilities observed in present-day machines varies from a steady-state saturated mode amplitude at nearly fixed frequency to a bursting amplitude and sweeping frequency scenarios.[4–6] Depending on the type of the nonlinear evolution, transport and peak loads of lost energetic particles to the wall vary significantly, so it is important to understand the key physics effects determining the type of the nonlinear evolution of waves excited by the energetic particles.

Since the energetic particle instabilities usually involve wave-particle resonant interaction, theory developments focus on the resonant particles. This approach simplifies the description of the multi-dimensional problem as the particle motion is effectively one-dimensional in the vicinity of a resonance if proper action-angle variables are employed.[7] A one-dimensional bump-on-tail model (see, e.g., Ref. 8 and references therein) was proven to be one of the most effective in describing the characteristic nonlinear scenarios in the past.[9–13] The corresponding cubic order equation has recently been solved for parameters taken directly from MHD simulations.[14] It was found[12,13] that the different types of nonlinear evolution of modes driven via wave-particle resonances can be attributed to the nature and the rate of the relaxation effects restoring the unstable distribution function of the energetic particles at the position of the resonance. In particular, it was shown that the relaxation of a dynamical friction type (for example electron drag for energetic ions) causes only the bursting evolution of the mode amplitude at a concomitant strong frequency sweeping, while a diffusive type relaxation may produce four types of nonlinear evolution: steady-state, periodic modulation of the mode amplitude (pitchfork splitting), chaotic evolution, and bursting evolution. This theory is in robust agreement with the observed Alfvén instabilities driven by the auxiliary heating ions on many tokamaks.

A surprising recent result from the TJ-II stellarator[15] was the observation of a change in the temporal evolution of a beam-driven Alfvén Eigenmode (AE) during rotational transform (iota) profile variation. In this experiment, AEs were excited by NBI-produced beam ions. As the iota varied throughout a single discharge, the AE nonlinear evolution was transformed from bursting to steady-state, and then to bursting again. During the iota variation, neither the density nor the temperature of the plasma changed significantly enough to affect the ratio between the drag and diffusion relaxation mechanisms restoring the beam distribution.

In this article, we point out that due to 3D configuration in the TJ-II machine, the same AE could resonate simultaneously with two distinctly different types of the beam ions, one of which is determined by a dominant drag, and the other one by pitch-angle scattering. As the nonlinear scenario of AE evolution is determined by two contributions from the types of beam ions with so different properties, the resulting type of the nonlinear scenario could be determined by the ratio between the resonating ions of the first and second types. We propose then that the role of the change in the iota profile is in a slight variation of the proportion between the beam ions of the first and second types, instead of the global changes in either T_e or n_e. This division of the resonant beam ions in two groups in TJ-II differs from other magnetic fusion devices and could be best explained via the unique shape of the TJ-II resonance map.

A resonance map of a typical mode, shown in Fig. 1, demonstrates how this specific TJ-II stellarator configuration gives rise to wave-particle resonances in two very different regions of the phase space. The guiding center particle orbits, starting on a core flux surface (normalized poloidal flux $\psi_N = 0.25$), have been simulated for experimental parameters of interest. The resonance function $F \equiv |n\omega_\phi - m\omega_\theta - \omega|$ is plotted as a function of the particles' energy and pitch-angle for a choice

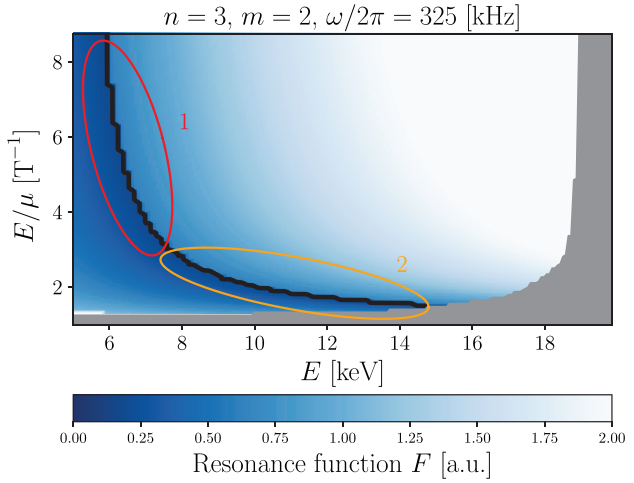

FIG. 1. Map of the resonance function $F \equiv |n\omega_\phi - m\omega_\theta - \omega|$ for energetic particles launched from $\psi_N = 0.25$ in TJ-II. The resonance condition $F = 0$ is highlighted by the black line. The grey region corresponds to particles on loss orbits. Two regions of interest along the resonance are indicated.

of toroidal and poloidal mode numbers $n = 3$, $m = 2$, respectively, for a wave with $f = 325$ kHz; a black line indicates the resonance condition $F = 0$. This very special shape of the resonance map suggests a natural division of the whole population of the fast ion resonant phase space into two regions. Region 1 (red oval) is narrow in energy ($6 < E < 8$ keV), but with appreciable variation in pitch-angle, while region 2 (orange oval) covers only a narrow range of pitch-angles and extends in energy ($8 < E < 14$ keV). In region 1, drag alone determines the replenishment of the distribution function at the resonance, while region 2 is determined by the pitch-angle scattering effect (diffusive collisional operator). Therefore, one arrives at the possibility of describing the nonlinear evolution of the AEs by a sum of two ion species with different weighting factors, one of which is dominated by drag and the other by diffusion. It is natural to assume that the iota variation affects the relative weight of each resonant ion species, and this may cause the experimentally observed change in nonlinear mode evolution.

II. TWO SPECIES MODEL

We consider a population of fast particles with a distribution F interacting with a wave through an electric field $E \sim \hat{E}\cos(kx - \omega t)$. We consider marginally unstable modes, with the linear growth rate and damping rate, respectively, satisfying $\gamma_L > \gamma_d \gg |\gamma_L - \gamma_d|$. We assume the distribution to satisfy the Fokker-Planck equation in one dimension given by

$$\frac{\partial F}{\partial t} + v\frac{\partial F}{\partial x} - \frac{|q|E}{m}\frac{\partial F}{\partial v} = \left.\frac{dF}{dt}\right|_{\text{coll}}. \tag{1}$$

This kinetic equation may be transformed into the frame of an electrostatic wave with wavenumber $k = 2\pi/\lambda$, by making the substitutions $\xi = kx - \omega t$ and $u = kv - \omega$, as follows:

$$\frac{\partial F}{\partial t} + u\frac{\partial F}{\partial \xi} - \frac{1}{2}\left(\omega_B^2 e^{i\xi} + \omega_B^{*2} e^{-i\xi}\right)\frac{\partial F}{\partial u} = \left.\frac{dF}{dt}\right|_{\text{coll}}. \tag{2}$$

Here, the electric field is represented by the fast particle nonlinear bounce frequency $\omega_B^2 = qk\hat{E}/m$ and other symbols have their usual meanings. The distribution function is decomposed as a Fourier series $F = F_0 + f_0 + \sum_{n=1}^{\infty}[f_n \exp(in\xi) + f_n^* \exp(-in\xi)]$; in a similar electric field decomposition, $\hat{E}$ is the $n = 1$ component. The collision term is taken to be[12]

$$\left.\frac{dF}{dt}\right|_{\text{coll}} = \alpha^2\frac{\partial F}{\partial u} + \nu^3\frac{\partial^2 F}{\partial u^2}, \tag{3}$$

where the α term corresponds to velocity-space friction and ν to diffusion. A complete set of equations is formed with the addition of Ampère's law, $\partial E/\partial t = -4\pi J$. The two terms making up the current are the perturbed bulk motion of the cold electrons (slowed by collisions $\propto \gamma_d$) and an integral over the fast electron distribution. For the resonant interaction with the wave,[13] this becomes

$$\frac{\partial \omega_B^2}{\partial t} = -\gamma_d\omega_B^2 + \frac{4\pi e^2\omega}{mk}\int f_1 du. \tag{4}$$

One approach to solve these equations to cubic order is to compare coefficients and integrate iteratively.[9,12] The electric field satisfies the following relation:

$$\frac{dA}{d\tau} = A - \frac{1}{2}\int_0^{\tau/2} dz\, z^2 A(\tau - z) \times \int_0^{\tau-2z} dx\, K(\hat{\alpha},\hat{\nu})A(\tau - z - x)A^*(\tau - 2z - x), \tag{5}$$

where $A = \omega_B^2[\gamma_L/(\gamma_L - \gamma_d)^5]^{1/2}$ and $\tau = (\gamma_L - \gamma_d)t$. The integral's kernel, arising from the collision operator, is given by

$$K(\hat{\alpha},\hat{\nu}) = \exp\left[i\hat{\alpha}^2 z(z + x) - \hat{\nu}^3 z^2(2z/3 + x)\right], \tag{6}$$

where the normalized coefficients $\hat{\alpha} = \alpha/(\gamma_L - \gamma_d)$, $\hat{\nu} = \nu/(\gamma_L - \gamma_d)$. It has previously been shown analytically[12] that for a single fast particle species to cubic order in electric field, a stable steady state exists only for $\hat{\nu} \geq 2$ and $\hat{\nu} > 1.043\hat{\alpha}$.

In this article, we consider two perturbative interacting distributions $F = F_0 + F_1 + F_2$, with

$$F_1 = f_{1,0} + \sum_{n=1}^{\infty}\left[f_{1,n}\exp(in\xi) + f_{1,n}^*\exp(-in\xi)\right] \tag{7}$$

and similarly for F_2. The collision operator acts on each distribution separately as follows:

$$\left.\frac{dF}{dt}\right|_{\text{coll}} = \sum_{j=1,2}\alpha_j^2\frac{\partial F_j}{\partial u} + \nu_j^3\frac{\partial^2 F_j}{\partial u^2}. \tag{8}$$

This operator arises from the differences in the sensitivity of the two groups of fast particles to changes in energy and pitch angle. To cubic nonlinearity, the kernel in Eq. (5) is split into two components

$$K_{\text{tot}} = \sum_{j=1,2} c_j K(\hat{\alpha}_j,\hat{\nu}_j), \tag{9}$$

where $K(\hat{\alpha}_j,\hat{\nu}_j)$ is an individual kernel from Eq. (6) and c_j is the relative weight of the respective distribution.

A two-species approach was previously developed for describing a near-threshold nonlinear evolution of a bump-on-tail instability, in which the energetic ion drive was balanced by the electron Landau damping.[16] In the corresponding generalization of the single species mode equation with cubic nonlinearity to the case of the mode interacting simultaneously with resonant species of very different mass (ions and electrons), the weights were shown to satisfy

$$c_j = \frac{\gamma_j r_j}{\gamma_L - \gamma_d}, \tag{10}$$

where for the species of type j, r_j is the mass-dependent coefficient, γ_j is the linear growth/damping rate, and K_j is the collisionality kernel. A similar approach is valid for our case of two particle species, but instead of the different masses considered in Ref. 16, different collisionality kernels K_j are the focus of our study.

Beyond the cubic nonlinearity model, the Bump On Tail (BOT) code[13] is another approach to efficiently solve the system of Eqs. (2) and (4) exactly by working in reciprocal space. We have modified it to permit two distributions, to explore the situation outlined earlier in the fully nonlinear regime. Each spatial harmonic of the distribution function is now Fourier transformed by an integral over velocity

$$\mathcal{G}_{j,n}(s) = \int f_{j,n} \exp\left(-isu/\gamma_L\right) du. \tag{11}$$

This approach simplifies Eq. (7) to a series of advection equations with a purely algebraic collision operator

$$\frac{\partial \mathcal{G}_{j,n}}{\partial \tau} - n\frac{\partial \mathcal{G}_{j,n}}{\partial s} - \frac{R_{j,n}}{\gamma_L^2} = \left(i\frac{\alpha_j^2}{\gamma_L^2}s - \frac{\nu_j^3}{\gamma_L^3}s^2\right)\mathcal{G}_{j,n}. \tag{12}$$

The velocity term is given by

$$R_{j,n} = \frac{is}{2}\left[\omega_B^2 \mathcal{G}_{j,n-1} + \omega_B^{*2}\mathcal{G}_{j,n+1}\right] + \omega_B^2 \delta(s)\delta_{n0}, \tag{13}$$

where δ represents the Dirac and Kronecker deltas respectively; for the $n=0$ term, the relation $\mathcal{G}_{j,-1}(s) = \mathcal{G}_{j,1}^*(-s)$ is used. Spatial harmonics up to the arbitrary order N required for convergence are computed.

The two distributions interact through the electric field described by the Fourier-space Ampère's law

$$\frac{\partial \omega_B^2}{\partial \tau} = -\frac{\gamma_d}{\gamma_L}\omega_B^2 + \frac{4\pi e^2 \omega}{mk\gamma_L}\sum_{j=1,2} c_j \mathcal{G}_{j,1}(0), \tag{14}$$

where the velocity integral has already been evaluated by taking the Fourier transform approach. Therefore, the coupled advective equations for each distribution function evolve separately as in the single distribution case, but interact through a common electric field.

III. STABILIZATION BY DIFFUSIVE DISTRIBUTION

It was previously shown[12] that the diffusion of a single fast particle distribution has a "stabilizing" effect on the nonlinear wave evolution. The wave amplitude does not exhibit explosive evolution, but instead saturates at some finite level. However, we now aim to demonstrate that the same effect can be achieved by a secondary, highly diffusive, population even when a more strongly weighted primary population determined by its drag does not permit a stable steady state solution. The relative weights of each distribution, which appear in Eqs. (9) and (14), c_1 and c_2, depend on the corresponding damping rate. Therefore, they are not set purely by the density of the respective population, and so a population with a relatively low proportion of particles can nonetheless have a significant effect on the wave evolution.

In Fig. 2(a), we show the electric field evolution for a single particle distribution with a choice of $\hat{\alpha} = 2$ and $\hat{\nu} = 2.5$, which evolves "explosively" outside the parameter space of stable solutions. We add a second, purely diffusive population with $\hat{\nu}_2^3 = 10\hat{\nu}_1^3$, which is stable alone; we impose a normalization condition by keeping $c_1 + c_2 = 1$ for the

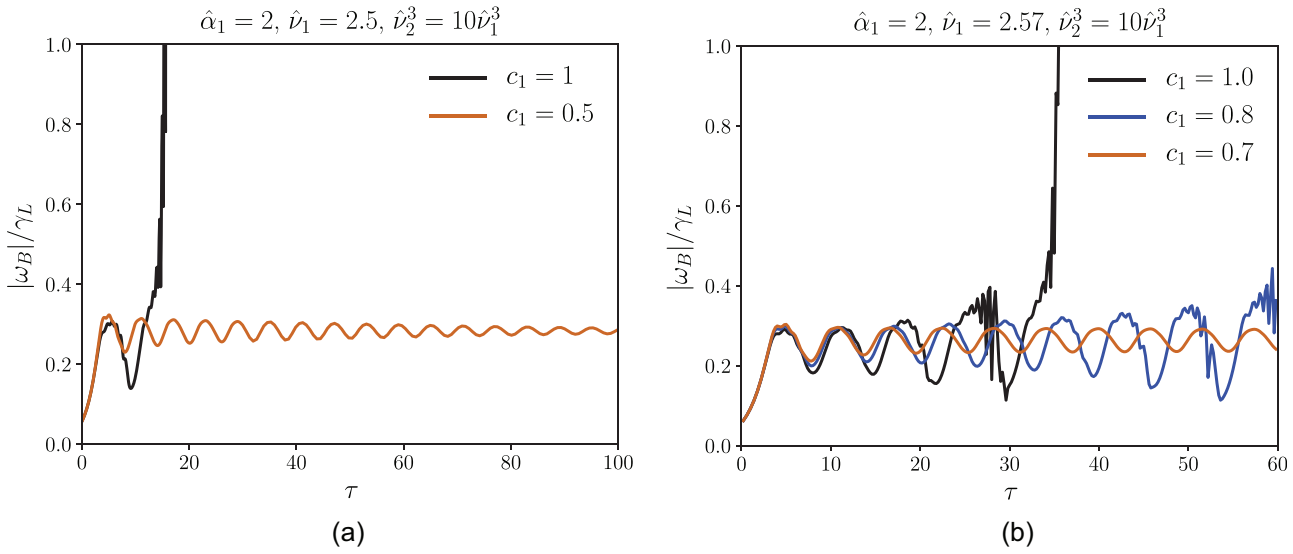

FIG. 2. Bounce frequency solved to cubic nonlinearity, showing "explosive" evolution (black curve) for a single particle population with a given value of drag and two of diffusion. This is stabilized by a second highly diffusive population (orange curve), with $c_1 + c_2 = 1$ in all cases. An intermediate case, where the explosive behavior occurs at a later time, is shown in the second panel.

rest of the article. The resulting solution is then stabilized to cubic order and tends to a constant value when the weights of the diffusive and destabilizing populations are of the same order. However, when the first distribution is moved closer to stability, the threshold for stabilization becomes lower, as expected; this is shown in Fig. 2(b). A transition is seen to occur from the electric field rapidly growing after only several oscillations ($c_1 = 1$), to growing over many oscillations ($c_1 = 0.8$), to the fully stable case ($c_1 = 0.7$). The choice of $\hat{\nu}_2$ in these cases reflects the properties of ions accelerated by Ion Cyclotron Resonant Heating (ICRH), where a strong quasilinear diffusion forms the energetic particle tail.[11]

This effect is observed also in the fully nonlinear case of the BOT code. We choose parameters that are unstable to cubic order and correspondingly show the characteristic often observed as hook-shaped structures[6] in the mode's frequency structure. A synthetic spectrogram showing these features for a choice of $\hat{\alpha}_1 = 1.5$ and $\hat{\nu}_1 = 1.4$ (also outside the cubic stability region) is shown in Fig. 3(a); we choose $\gamma_d = 0.9\gamma_L$ throughout this article. In this case, the addition of a second "ICRH" distribution with $c_2 = 0.5$ causes a transition from the chaotic oscillations in the electric field (which leads to the frequency behavior mentioned earlier) to a much more regular, long-scale oscillations whose corresponding spectrogram is shown in Fig. 3(b). For a purely diffusive distribution, after a short initial period of oscillations, the electric field saturates to a constant value.

These classes of mode evolution can be understood through the resulting form of the distribution function, which appears in Eq. (7). A purely diffusive collisional operator acts to flatten the distribution function and create a plateau around the resonance $u = 0$, leading to the saturation of the electric field as outlined earlier. The addition of drag to the collisional operator leads to the formation of holes and clumps in the distribution function and the corresponding asymmetric structures in the resulting spectrogram. The distribution functions are shown to the leading two orders (the background F_0 and the dominant $\sum_{j=1,2} c_j f_{j,0}$ term), at one time point $\tau \equiv t\gamma_L = 50$ of the BOT simulation detailed above, are shown in Fig. 4. The term involving the sum influences the evolution of the bounce frequency through its Fourier transform in Ampere's law, Eq. (14).

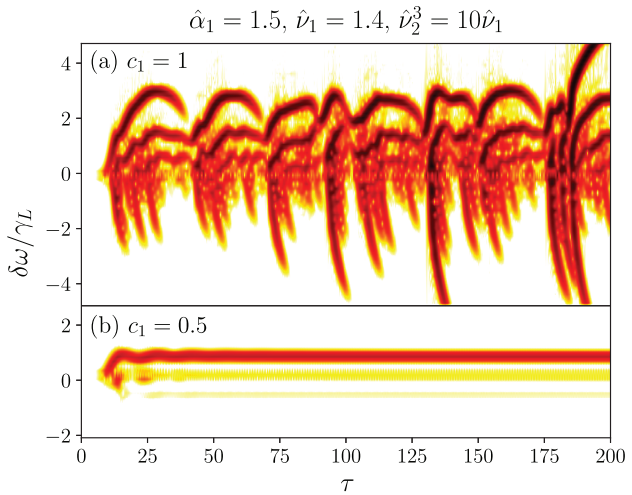

FIG. 3. Synthetic spectrograms from nonlinear BOT simulations with parameters as indicated, showing (a) chirping evolution and (b) stabilization by a second diffusive distribution.

We have analyzed the velocity space coefficients of the two regions of interest of the TJ-II resonance map in Fig. 1 with the Fokker-Planck approach.[17] We consider the experimental plasma parameters in the expression for the velocity space resonance. As shown in the Appendix, we estimate that the drag of the 6–8 keV beam (region 1 in the resonance map) and the 10–16 keV beam pitch-angle scattering corresponding to diffusion (region 2) satisfy

$$\frac{\nu}{1.7} \approx \frac{\alpha}{3}. \tag{15}$$

By the same analysis, we confirm that drag in the first region dominates over diffusion and vice versa. We conjecture that the role of the magnetic configuration in the TJ-II experiment is in slightly shifting the proportion of the fast ions in region 1 with respect to that in region 2.

Two regimes are seen in BOT simulations depending on the choice of c_1 and c_2 (which are taken to satisfy $c_1 + c_2 = 1$), as shown in Fig. 5. A synthetic spectrogram of the electric field is shown for the drag-dominated case, with distinct branches sweeping upwards in frequency, many comparatively small branches sweeping downwards and the periodic broadband noise bursts. The frequency asymmetry arises due to the nature of the drag term. As the weight of the diffusion term is increased, such rapid oscillations disappear and the amplitude saturates to a constant value. Hence, there is no frequency sweep; low-frequency bursts, such as that seen around $\tau = 175$, appear sporadically with long time separation.

IV. CONCLUSION

A two-species model with two different relaxation effects was developed for describing the near-threshold nonlinear evolution of the beam-driven AEs. Within the lowest-order

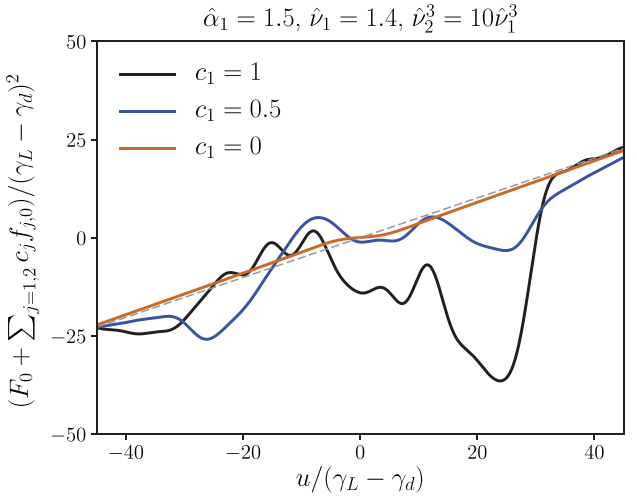

FIG. 4. The two leading terms of the distribution functions, as defined in Eq. (7), computed by BOT at $\tau = 50$ for the simulations presented in Fig. 3. In the cases with velocity-space drag, the formation of several holes and clumps can be seen, which travel outwards. The dashed grey line corresponds to the unperturbed distribution.

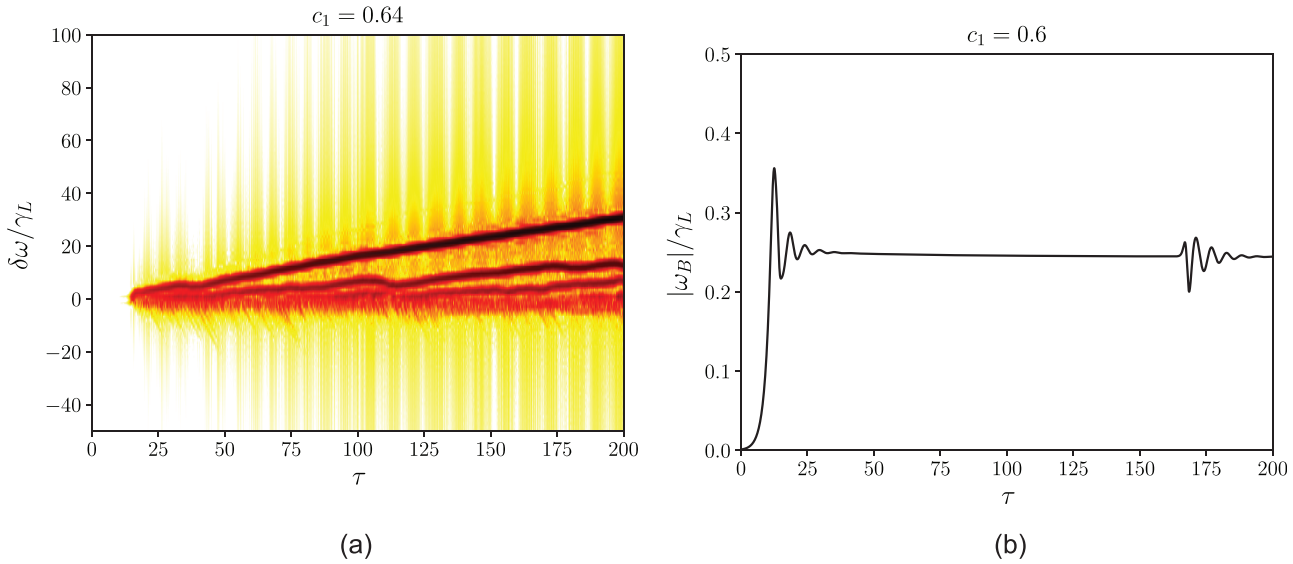

FIG. 5. Cases with two distributions of fast particles, one with drag $\hat{\alpha}_1 = 4.5$ and one with diffusion $\hat{\nu}_2 = 2.55$. (a) With a relatively low proportion of the diffusion distribution, $c_1 = 0.64$ ($c_1 + c_2 = 1$ in both cases) a spectrogram of ω_B shows the formation of several frequency sweeping branches. (b) As the diffusive proportion is increased to $c_2 = 0.4$, the activity is stabilized, with the amplitude saturating and $\delta\omega \approx 0$.

cubic nonlinear equation, a possibility of transforming the explosive AE scenario driven by the energetic particles with drag relaxation into a steady-state AE by adding a second species term with diffusion relaxation was demonstrated. For investigating the nonlinear AE evolution beyond the cubic nonlinearity, a two-species BOT code was developed. The results of the BOT modelling show a wide variety of nonlinear regimes including the steady-state ones and bursting, controlled by the proportion between the first and second species. The results suggest that it may be possible to control the nonlinear evolution of alpha particle-driven AEs in ITER by adding ICRH-accelerated ions with dominant quasi-linear diffusive relaxation.

The resonance map obtained for the interaction of beam ions with AEs in the TJ-II stellarator suggests two very different regions of the resonant beam phase space: the first with dominant drag relaxation and the second with dominant pitch-angle diffusive relaxation. This model may explain the experimentally observed TJ-II results, as variation in the rotational transform changes the relative weights of the two beam species. The observed correlation between the type of nonlinear AE evolution and the magnetic configuration may be caused by a number of effects going beyond the assumptions used in the 1 D Bump-On-Tail model. The most essential assumptions are: (1) the damping of the mode does not change throughout the mode evolution; (2) no other free energy source exists apart from the energetic particle drive (*e.g.,* the MHD part playing a role in fishbones is excluded); (3) the width of the resonance is much smaller than the width of the mode (as the width of the mode is not present in the 1 D bump-on-tail model).

ACKNOWLEDGMENTS

This work has been part-funded by the RCUK Energy Programme [Grant No. EP/P012450/1]. Support from the U.S. group was provided by the U.S. DOE under Grant No DE-FG02–99ER54563.

APPENDIX: FOKKER-PLANCK EVOLUTION OF THE BEAM DISTRIBUTION FUNCTION

For AE modes driven by the NBI-produced energetic ions in plasmas with parameters similar to those in the TJ-II machine, Coulomb relaxation only plays a role in shaping the unstable distribution function. The drag and diffusion relaxation at the wave-particle resonance could be assessed from a Fokker-Planck approach as follows. Consider the temporal evolution of an energetic particle beam distribution function, $F_b(u, \lambda, \tau)$, in the presence of Coulomb collisions with thermal plasma species (beam-beam collisions are neglected). No AE effect on the fast ions is considered. The Fokker-Planck equation for the beam distribution function with initial velocity V_0 in the range between thermal ion and thermal electron velocities, $\nu_i \ll V_0 \ll \nu_e$, can be represented in the form (see *e.g.,* Ref. 17)

$$\frac{dF_b}{d\tau} - \frac{1}{u^2}\frac{\partial}{\partial u}\left[(1+u^3)F_b\right] - \frac{A}{2u^3}\frac{\partial}{\partial\lambda}(1-\lambda^2)\frac{\partial F_b}{\partial\lambda} = S - \nu_s F_b, \tag{A1}$$

where

$$u = V/V_I, \tag{A2}$$

$$\lambda = V_\parallel/V, \tag{A3}$$

$$\tau = \nu t, \tag{A4}$$

$$V_I^3 = \frac{3\sqrt{\pi}}{4}\frac{m_e}{m_b}\nu_e^3\tilde{Z}, \tag{A5}$$

$$\nu = 4\pi\frac{n_0 e^4 \tilde{Z}\ln\Lambda}{m_b V_I^3}, \tag{A6}$$

$$A = Z_{eff}/\tilde{Z}, \tag{A7}$$

$$Z_{eff} = \sum_i Z_i^2 n_i/n_0, \tag{A8}$$

$$\tilde{Z} = \frac{m_b}{n_0}\sum_i Z_i^2 n_i/m_i. \tag{A9}$$

Here, $S(u,\lambda,\tau)$ is the beam source, $\nu_s F_b$ represents a sink of the energetic ions, V_I is the critical velocity at which the heating power from the beam to electrons equals that to the thermal ions, $\ln\Lambda$ is the Coulomb logarithm, m_b, m_e m_i, are the beam, thermal electron, and ion masses, n_i are thermal ion densities, and the electron density satisfies $n_0 = \sum_i Z_i n_i$. The effect of Coulomb diffusion on the temporal evolution of $F_b(u,\lambda,\tau)$ is given by the pitch-angle scattering term, the last one in the left-hand-side of Eq. (A1). The effect of the drag is represented by the second term in the left-hand-side of Eq. (A1). For plasmas with parameters of the TJ-II machine,[15] *i.e.*, $n_0 \approx 10^{13}$ cm^{-3}, $T_e \approx 400$ eV, and hydrogen species of both the beam and the plasma, $m_b = m_i = m_H$, $Z_b = Z_i = 1$, satisfying $n_b \ll n_i$, one obtains

$$\nu_e \approx 1.2\times 10^9 \text{ cm s}^{-1};\quad Z_{eff}\approx 1;\quad \tilde{Z}\approx 1;$$
$$V_I^3 \approx 7.3\times 10^{-4}\nu_e^3;\quad \nu \approx 32\,\text{s}^{-1}. \tag{A10}$$

In the normalized units of Eqs. (A2)–(A9), the estimates (A10) give maximum and minimum values of the beam velocity and the beam pitch-angle for the resonance regions shown in Fig. 1. For region 1 with $6\,\text{keV} \le E_b \le 8$ keV

$$u_b^{min}\approx 2;\ u_b^{max}\approx 2.54;\ \rho_b^{min}\approx 3;\ \rho_b^{max}\approx 8, \tag{A11}$$

where $\rho \equiv E/\lambda$. For region 2 with $10\,\text{keV} \le E_b \le 16$ keV

$$u_b^{min}\approx 2.8;\ u_b^{max}\approx 3.6;\ \rho_b^{min}\approx 2;\ \rho_b^{max}\approx 3. \tag{A12}$$

The slowing-down time of the beam from u_b^{max} to u_b^{min} could be estimated as[17]

$$\tau_{SD} = \frac{1}{3}\ln\left[\frac{1+(u_b^{max})^3}{1+(u_b^{min})^3}\right] \approx 2.8\times 10^{-3}, \tag{A13}$$

which corresponds to $t_{SD}\approx 9\times 10^{-5}$ s. For the pitch-angle scattering dominant in region 2, the following expression could be employed:

$$\frac{1}{\rho_b^{min}} - \frac{1}{\rho_b^{max}} = \frac{A}{3}\ln\left[1+\frac{1-\exp(-3\tau)}{u^3}\right], \tag{A14}$$

which gives the characteristic time of the pitch-angle scattering across the resonance in the region 2 then as $\tau_{scat}\approx 6\times 10^{-3}$, corresponding to $t_{scat}\approx 2\times 10^{-4}$ s.

The characteristic times in Eqs. (A13) and (A14) could be normalized by the instability characteristic time, e.g., by assuming the net growth rate to be $\gamma_L - \gamma_d$. For the observed AE at $\omega \approx 300$ kHz the normalized slowing-down time across the resonance in region 1 is then

$$\frac{2\pi\alpha}{\gamma_L-\gamma_d}\approx 3, \tag{A15}$$

while the normalised pitch-angle scattering time in region 2 is

$$\frac{2\pi\nu}{\gamma_L-\gamma_d}\approx 1.7. \tag{A16}$$

A value of $\gamma_d = 0.9\gamma_L$ is used in the calculations above, while γ_L remains a free parameter.

[1]A. Fasoli, C. Gormenzano, H. L. Berk, B. N. Breizman, S. Briguglio, D. S. Darrow, N. N. Gorelenkov, W. W. Heidbrink, A. Jaun, S. V. Konovalov, R. Nazikian, J.-M. Noterdaeme, S. E. Sharapov, K. Shinohara, D. Testa, K. Tobita, Y. Todo, G. Vlad, and F. Zonca, Nucl. Fusion **47**, S264 (2007).
[2]ITER Physics Expert Group on Energetic Particles, Heating and Current Drive and ITER Physics Basis Editors, Nucl. Fusion **39**, 2471 (1999).
[3]H. H. Duong, W. W. Heidbrink, E. J. Strait, T. W. Petrie, R. Lee, R. A. Moyer, and J. G. Watkins, Nucl. Fusion **33**, 749 (1993).
[4]S. E. Sharapov, B. Alper, H. L. Berk, D. N. Borba, B. N. Breizman, C. D. Challis, I. G. J. Classen, E. M. Edlund, J. Eriksson, A. Fasoli, E. D. Fredrickson, G. Y. Fu, M. Garcia-Munoz, T. Gassner, K. Ghantous, V. Goloborodko, N. N. Gorelenkov, M. P. Gryaznevich, S. Hacquin, W. W. Heidbrink, C. Hellesen, V. G. Kiptily, G. J. Kramer, P. Lauber, M. K. Lilley, M. Lisak, F. Nabais, R. Nazikian, R. Nyqvist, M. Osakabe, C. Perez von Thun, S. D. Pinches, M. Podesta, M. Porkolab, K. Shinohara, K. Schoepf, Y. Todo, K. Toi, M. A. Van Zeeland, I. Voitsekhovich, R. B. White, V. Yavorskij, E. P. T. G. ITPA, and J. E. T. EFDA, Contributors, Nucl. Fusion **53**, 104022 (2013).
[5]S. D. Pinches, H. L. Berk, M. P. Gryaznevich, S. E. Sharapov, and JET-EFDA Contributors Plasma Phys. Controlled Fusion **46**, S47 (2004).
[6]H. L. Berk, C. J. Boswell, D. Borba, A. C. A. Figueiredo, T. Johnson, M. F. F. Nave, S. D. Pinches, S. E. Sharapov, and JET EFDA Contributors, Nucl. Fusion **46**, S888 (2006).
[7]A. N. Kaufman, Phys. Fluids **15**, 1063 (1972).
[8]A. I. Akhiezer, I. A. Akhiezer, R. V. Polovin, A. G. Sitenko, and K. N. Stepanov, *Plasma Electrodynamics* (Pergamon Press, Oxford, 1975).
[9]H. L. Berk, B. N. Breizman, and M. Pekker, Phys. Rev. Lett. **76**, 1256 (1996).
[10]H. L. Berk, B. N. Breizman, and M. S. Pekker, Plasma Phys. Rep. **23**, 778 (1997).
[11]A. Fasoli, B. N. Breizman, D. Borba, R. F. Heeter, M. S. Pekker, and S. E. Sharapov, Phys. Rev. Lett. **81**, 5564 (1998).
[12]M. K. Lilley, B. N. Breizman, and S. E. Sharapov, Phys. Rev. Lett. **102**, 195003 (2009).
[13]M. K. Lilley, B. N. Breizman, and S. E. Sharapov, Phys. Plasmas **17**, 092305 (2010).
[14]V. N. Duarte, H. L. Berk, N. N. Gorelenkov, W. W. Heidbrink, G. J. Kramer, R. Nazikian, D. C. Pace, M. Podestà, B. J. Tobias, and M. A. Van Zeeland, Nucl. Fusion **57**, 054001 (2017).
[15]A. V. Melnikov, L. G. Eliseev, E. Ascasíbar, A. Cappa, F. Castejón, C. Hidalgo, T. Ido, J. A. Jiménez3, A. S. Kozachek, L. I. Krupnik, M. Liniers, S. E. Lysenko, K. Nagaoka, J. L. de Pablos, A. Shimizu, S. E. Sharapov, M. V. Ufimtsev, S. Yamamoto, HIBP Group and TJ-II Team, Nucl. Fusion **56**, 076001 (2016).
[16]H. L. Berk, B. N. Breizman, J. Candy, M. Pekker, and N. V. Petviashvili, Phys. Plasmas **6**, 3102 (1999).
[17]H. L. Berk, W. Horton, M. N. Rosenbluth, and P. H. Rutherford, Nucl. Fusion **15**, 819 (1975).